arXiv:1311.6701v2 [physics.atom-ph] 10 Dec 2013

Electric dipole moment of ^{129}Xe atom

[1]Yashpal Singh, [1]B. K. Sahoo* and [2]B. P. Das
[1] *Theoretical Physics Division, Physical Research Laboratory, Navrangpura, Ahmedabad - 380009, India and*
[2] *Theoretical Physics and Astrophysics Group, Indian Institute of Astrophysics, Bangalore-560034, India*

The parity (P) and time-reversal (T) odd coupling constant associated with the tensor-pseudotensor (T-PT) electron-nucleus interaction and the nuclear Schiff moment (NSM) have been determined by combining the result of the measurement of the electric dipole moment (EDM) of ^{129}Xe atom and calculations based on the relativistic coupled-cluster (RCC) theory. Calculations using various relativistic many-body methods have been performed at different levels of approximation and their accuracies are estimated by comparing the results of the calculated dipole polarizability of the ground state of the above atom with its most precise available experimental data. The non-linear terms that arise in the RCC theory at the singles and doubles approximation were found to be crucial for achieving high accuracy in the calculations. Our results for the ^{129}Xe EDM due to the odd T-PT interaction and the NSM are, respectively, $d_A = 0.501 \times 10^{-20} C_T \langle \sigma_N \rangle |e|cm$ and $d_A = 0.336 \times 10^{-17} \frac{S}{|e|\ fm^3} |e|cm$. These results in combination with the future EDM measurements in atomic Xe could provide the most accurate limits for the T-PT coupling constant and NSM.

PACS numbers:

The search for the electric dipole moment (EDM) is now in its seventh decade [1, 2]. The observation of an EDM of an elementary particle or a composite system would be an unambiguous signature of the violations of parity (P) and time-reversal (T) symmetries. T violation implies charge conjugation-parity (CP) violation via the CPT theorem [3]. The standard model (SM) of elementary particle physics provides explanations of the experimentally observed hadronic CP violation in the decays of neutral K [4] and B [5–7] mesons, but the amount of CP violation predicted by the SM is not sufficient to account for the matter-antimatter asymmetry in the Universe [8]. The current limits for CP violating coupling constants deduced from the atomic EDMs are several orders of magnitude higher than the predictions of these quantities by the SM [9–11]. In addition, atomic EDMs can probe CP violation originating from leptonic, semi-leptonic and hadronic CP sources. Combining atomic EDM measurements with high precision many-body calculations, it is possible to obtain various CP violating coupling constants at the levels of the nucleus and the electron. Newly proposed EDM experiments on diamagnetic and paramagnetic atoms hold the promise of improving the sensitivity of the current measurements by at least a few orders of magnitude [12–16]. The EDMs of diamagnetic atoms arise predominantly from the electron-nucleus tensor-pseudotensor (T-PT) interaction and interaction of electrons with the nuclear Schiff moment (NSM) [17]. The electron-nucleus T-PT interaction is due to the CP violating electron-nucleon interactions which translates to CP violating electron-quark interactions at the level of elementary particles. The NSM on the other hand could exist due to CP violating nucleon-nucleon interactions and the EDM of nucleons and both of them in turn could originate from CP violating quark-quark interactions or EDMs and chromo EDMs of quarks. In order to obtain precise limits for the coupling constants of these interactions and EDMs of quarks, it is necessary to perform both experiments and calculations as accurately as possible on suitable atoms.

To date the best limit for a diamagnetic atomic EDM is obtained from ^{199}Hg atom as $d_A < 3.1 \times 10^{-29}\ |e|cm$ [18] and the next best limit comes from an earlier measurement on ^{129}Xe atom as $d_A < 4.1 \times 10^{-27}\ |e|cm$ [19]. Both ^{129}Xe and ^{199}Hg isotopes are good choices for carrying out EDM measurements as they have nuclear spin $I = 1/2$ and therefore the interaction with the octupole moment vanishes. Owing to the fact that the matrix elements of the T-PT and NSM interaction Hamiltonians increase with the size of the atomic system, their enhancements in atomic Hg are larger than Xe. However, the new proposals on EDM measurements in ^{129}Xe argue in favor of carrying out the experiment in this isotope because of its larger spin relaxation time [13]. As a matter of fact, three research groups around the world are now actively involved in Xe EDM experiments [13, 20, 21]. Inoue *et al.* have proposed to utilize the nuclear spin maser technique [22] to surpass the limit provided by the Hg EDM measurement.

In this Letter, we report the results of our systematic theoretical studies of the P- and T- odd coupling constant for the T-PT interaction and of the NSM in ^{129}Xe. To this end, we have developed many-body methods in the framework of the third order many-body perturbation theory (MBPT(3)) for a better understanding of the different classes of correlation effects, the coupled-perturbed-Hartree-Fock (CPHF) method in order to reproduce the previously reported results and the relativistic coupled-cluster (RCC) theory to bring to light the

*bijaya@prl.res.in

TABLE I: Results of α in ea_0^3, $\overline{\eta} = 10^{20} \times \eta$ and $\overline{\zeta} = 10^{17} \times \zeta$ for the ground state of Xe using different many-body methods. The CCSD results given in bold fonts are the recommended values from the calculations on the physical ground.

Method of	This work			Others			
Evaluation	α	$\overline{\eta}$	$\overline{\zeta}$	α	$\overline{\eta}$	$\overline{\zeta}$	Ref.
DF	26.918	0.447	0.288		0.45	0.29	[23]
MBPT(2)	23.388	0.405	0.266				
MBPT(3)	18.693	0.515	0.339		0.52		[24]
CPHF	26.987	0.562	0.375		0.57	0.38	[23]
				27.7	0.564		[25]
LCCSD	27.484	0.608	0.417				
CCSD	**27.744**	**0.501**	**0.336**				
Experiment	27.815(27)						[26]

roles of both the CPHF and non-CPHF contributions (e.g. pair-correlation effects) to all orders in the residual Coulomb interaction (difference between the exact two-body Coulomb and the mean-field interactions). In the present work, we consider only one hole-one particle and two hole-two particle excitations, i.e. the CCSD method and its linearized approximation, the LCCSD method. The ground state of a closed shell atom like Xe can be exactly described in the RCC theory by

$$|\Psi\rangle \;=\; e^T|\Phi_0\rangle, \tag{1}$$

where the cluster operator T generates single and double excitations from the Dirac-Hartree-Fock (DF) wave function $|\Phi_0\rangle$ by defining $T = T_1 + T_2$. These operators can be expressed in second quantization notation using hole and particle creation and annihilation operators as

$$T_1 = \sum_{a,p} a_p^\dagger a_a t_a^p \;\;\text{and}\;\; T_2 = \frac{1}{4}\sum_{a,b,p,q} a_p^\dagger a_q^\dagger a_b a_a t_{ab}^{pq} \tag{2}$$

with t_a^p and t_{ab}^{pq} are the excitation amplitudes from the occupied orbitals denoted by a, b to the unoccupied orbitals denoted by p, q which embody correlation effects among the electrons to all orders. We consider the Dirac-Coulomb (DC) Hamiltonian which in atomic unit (au) is given by

$$H \;=\; \sum_i [c\boldsymbol{\alpha_D}\cdot\mathbf{p}_i + (\beta_D - 1)c^2 + V_n(r_i)] + \sum_{i,j>i}\frac{1}{r_{ij}}, \tag{3}$$

where c is the velocity of light in vacuum, α_D and β_D are the Dirac matrices, V_n denotes the nuclear potential obtained using the Fermi-charge distribution and $\frac{1}{r_{ij}}$ is the dominant inter-electronic Coulombic repulsion. We also take into account one order of an additional operator H_{add} which is either the dipole operator D for the evaluation of dipole polarizability (α) or the P- and T-violating interaction Hamiltonians for determining their corresponding couplings coefficients. The T-PT and the NSM interaction Hamiltonians are given by [23]

$$H_{EDM}^{TPT} = \frac{iG_F C_T}{\sqrt{2}}\sum \boldsymbol{\sigma_n}\cdot\boldsymbol{\gamma_D}\rho_n(r) \tag{4}$$

and

$$H_{EDM}^{NSM} = \frac{3\mathbf{S}.\mathbf{r}}{B_4}\rho_n(r), \tag{5}$$

respectively, with G_F is the Fermi coupling constant, C_T is the T-PT coupling constant, $\boldsymbol{\sigma_n} = \langle\sigma_n\rangle\frac{\mathbf{I}}{I}$ is the Pauli spinor of the nucleus for the nuclear spin I, $\boldsymbol{\gamma_D}$ represents the Dirac matrices, $\rho_n(r)$ is the nuclear density, $\mathbf{S} = S\frac{\mathbf{I}}{I}$ is the NSM and $B_4 = \int_0^\infty dr r^4\rho_n(r)$.

To distinguish between the correlations only due to the Coulomb and the combined Coulomb and the additional interaction, we further define

$$T = T^{(0)} + T^{(1)} \tag{6}$$

for the cluster operators $T^{(0)}$ and $T^{(1)}$ that account for the correlations only due to the Coulomb interaction and the combined Coulomb-additional interactions respectively. To ensure the inclusion of only one order of the additional interaction in the wave function, we express

$$\begin{aligned}|\Psi\rangle \;&\simeq\; \left(e^{T^{(0)}} + e^{T^{(0)}}T^{(1)}\right)|\Phi_0\rangle \\ &=\; |\Psi^{(0)}\rangle + |\Psi^{(1)}\rangle,\end{aligned} \tag{7}$$

where $|\Psi^{(0)}\rangle$ and $|\Psi^{(1)}\rangle$ are the unperturbed and the first order perturbed wave functions due to the additional interaction. Owing to the nature of the additional operators, the first order perturbed wave function is an admixture of both the even and odd parities. The working equations for evaluating the excitation amplitudes of these RCC operators are described in [27].

Using the generalized Bloch equation, we can also express [27]

$$\begin{aligned}|\Psi\rangle \;&=\; \Omega^{(0)}|\Phi_0\rangle + \Omega^{(1)}|\Phi_0\rangle \\ &=\; \sum_k[\Omega^{(k,0)} + \Omega^{(k,1)}]|\Phi_0\rangle,\end{aligned} \tag{8}$$

where the Ωs are known as the wave operators with $\Omega^{(0,0)} = 1$ and $\Omega^{(1,0)} = H_{add}$ and k represents the order of interactions due to the Coulomb repulsion. In the MBPT(3) method, we restrict k up to 2. The diagrams that make important contributions in this approximation are given explicitly in [27]. In the CPHF method, we consider $\Omega^{(k,0)} \approx \Omega^{(0,0)}$ and $\Omega^{(k,1)}$ is evaluated to infinite order by restricting it only to one hole-one particle excitations by defining

$$\begin{aligned}\Omega_{a\to p}^{(\infty,1)} \;=\; \sum_{k=1}^{\infty}\sum_{b,q}\{&\frac{[\langle pb|\frac{1}{r_{ij}}|aq\rangle - \langle pb|\frac{1}{r_{ij}}|qa\rangle]\Omega_{b\to q}^{(k-1,1)}}{\epsilon_a - \epsilon_p} \\ &+\frac{\Omega_{b\to q}^{(k-1,1)^\dagger}[\langle pq|\frac{1}{r_{ij}}|ab\rangle - \langle pq|\frac{1}{r_{ij}}|ba\rangle]}{\epsilon_a - \epsilon_p}\},\end{aligned} \tag{9}$$

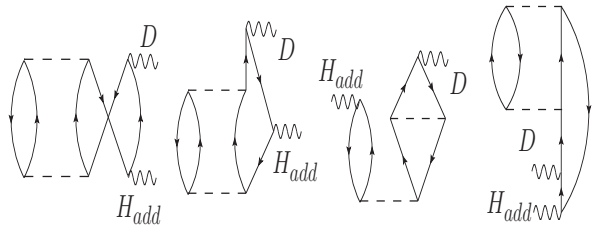


FIG. 1: Example of few dominant non-CPHF diagrams from the MBPT(3) method involving D and the corresponding perturbed interaction operator H_{add}.

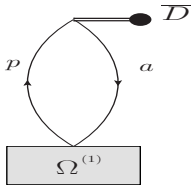


FIG. 2: Diagram involving effective one-body dipole operator $\overline{D}$ and the perturbed wave operator $\Omega^{(1)}$ that accounts for the contributions from the singly excited configurations.

TABLE II: Explicit contributions to the α in ea_0^3, $\overline{\eta} = 10^{20} \times \eta$ and $\overline{\zeta} = 10^{17} \times \zeta$ values from various CCSD terms.

Term	α	$\overline{\eta}$	$\overline{\zeta}$
$\overline{D}T_1^{(1)} + c.c$	26.246	0.506	0.338
$T_1^{(0)\dagger}\overline{D}T_2^{(1)} + c.c$	0.008	$\sim$0	$\sim$0
$T_2^{(0)\dagger}\overline{D}T_2^{(1)} + c.c$	1.395	-0.005	-0.001
$Extra$	0.095	$\sim$0	-0.001

with $\Omega_{a\rightarrow p}^{(0,1)} = -\frac{\langle p|H_{add}|a\rangle}{\epsilon_p - \epsilon_a}$, ϵ's are the orbital energies and $a \rightarrow p$ represents single excitations from $|\Phi_0\rangle$ by replacing one of its occupied orbitals a by a virtual orbital p.

Using the many-body tools discussed above, we evaluate X representing polarizability α, $\eta = \frac{d_A}{\langle\sigma_N\rangle C_T}$ or $\zeta = \frac{d_A}{S/(|e|\ fm^3)}$ by considering the appropriate additional operator using the general expression

$$X = 2\frac{\langle\Psi^{(0)}|D|\Psi^{(1)}\rangle}{\langle\Psi^{(0)}|\Psi^{(0)}\rangle}. \quad (10)$$

In the MBPT(3) method, we have

$$X = 2\frac{\sum_{k=0}^{m=k+1,2}\langle\Phi_0|\Omega^{(m-k-1,0)^\dagger}D\Omega^{(k,1)}|\Phi_0\rangle}{\sum_{k=0}^{m=k+1,2}\langle\Phi_0|\Omega^{(m-k-1,0)^\dagger}\Omega^{(k,0)}|\Phi_0\rangle}. \quad (11)$$

Therefore, the lowest order MBPT(1) with $k = 0$ corresponds to the DF approximation and the intermediate MBPT(2) approximation follows with $k = 1$.

The above expression yields the forms $X = 2\langle\Phi_0|\{D\Omega^{(\infty,1)}\}_{con}|\Phi_0\rangle$ in the CPHF method and $X = 2\langle\Phi_0|\{\overbrace{D}T^{(1)}\}_{con}|\Phi_0\rangle$ in the RCC theory with $\overbrace{D} = (1 + T^{(0)^\dagger})D$ in the LCCSD method and $\overbrace{D} = e^{T^{(0)^\dagger}}De^{T^{(0)}}$ is a non-truncating series in the CCSD method. The subscript *con* implies that all the terms inside the curly bracket are connected. We have described in an earlier work the procedure for evaluating the diagrams that make the dominant contributions to $\overbrace{D}$ [27].

We calculate α for the ground state of Xe by the methods mentioned above to test their accuracies. The most precise measured value of this quantity is reported as 27.815(27) ea_0^3 [26]. In Table I, we present the calculated α, η and ζ values along with the experimental and previously reported results. As can be seen from this table the DF result for α is close to the experimental result, but this is not the case when correlation effects are added via the MBPT(2) and MBPT(3) methods. The results of the all order CPHF, LCCSD and CCSD methods are in good agreement with the measured value, but the CCSD result is more accurate than the former two methods. The rationale for considering the non-linear RCC terms in the singles and doubles approximation for the precise evaluation of the ground state properties of Xe atom is therefore justified. It is also significant to note that the EDM enhancement factors exhibit different correlation trends than those of polarizability. The results increase gradually from the DF level after the inclusion of the correlation effects in the passage from the MBPT to LCCSD, and after that they decrease at the CCSD level. With reference to the α calculations, the CCSD results, which are marked in bold fonts in the above table, are clearly the most accurate. This is evident on physical grounds.

The results of calculations by others for α, η and ζ [23–25] as well as the methods used to calculate them are also given in Table I. As can be seen in that table, we have successfully reproduced the results of the previous calculations at the same level of approximation and we have gone beyond these approximations for obtaining accurate results. We present our results performing the calculations using the MBPT(3), LCCSD and CCSD methods in Table I. These results provide useful insights into the role of different types of correlation effects. From the MBPT(3) calculations, we find that certain non-CPHF type diagrams, for example the diagrams shown in Fig. 1, contribute substantially with opposite signs to those of the DF values in all the above quantities leading to large cancellations in the final results. Indeed this is the main reason why the CPHF method over estimates the EDM enhancement factors compared to the CCSD method. In fact many of these MBPT(3) diagrams correspond to the non-linear terms of the CCSD method, hence their contributions are absent in the LCCSD method. Therefore, the LCCSD method also over estimates these results even though they account for some of the lower order non-

TABLE III: Contributions from various matrix elements and from various angular momentum symmetry groups at the DF, lowest order CPHF (denoted by MBPT(l-CPHF)), CPHF and CCSD methods to the α in ea_0^3, $\overline{\eta} = 10^{20} \times \eta$ and $\overline{\zeta} = 10^{17} \times \zeta$ values. Here the summation indices n and m represent for the occupied and unoccupied orbitals, respectively.

Excitation(s)	DF			MBPT(l-CPHF)			CPHF			CCSD		
$(a \rightarrow p)$	α	$\overline{\eta}$	$\overline{\zeta}$	α	$\overline{\eta}$	$\overline{\zeta}$	α	$\overline{\eta}$	$\overline{\zeta}$	α	$\overline{\eta}$	$\overline{\zeta}$
$5p_{1/2} - 7s$	0.248	0.030	0.007	0.336	0.056	0.016	0.380	0.062	0.016	0.352	0.050	0.014
$5p_{1/2} - 8s$	0.517	0.090	0.022	0.690	0.159	0.045	0.769	0.172	0.045	0.733	0.145	0.039
$5p_{1/2} - 9s$	0.237	0.106	0.025	0.284	0.166	0.044	0.301	0.174	0.044	0.309	0.157	0.041
$5p_{3/2} - 7s$	0.844	$\sim$0	0.015	1.136	0.005	0.036	1.314	0.007	0.036	1.202	0.001	0.031
$5p_{3/2} - 8s$	1.558	$\sim$0	0.043	2.056	0.014	0.093	2.351	0.018	0.093	2.261	0.024	0.082
$5p_{3/2} - 9s$	0.583	$\sim$0	0.044	0.678	0.012	0.081	0.745	0.015	0.081	0.809	0.017	0.076
$5p_{1/2} - 7d_{3/2}$	2.267	$\sim$0	$\sim$0	2.200	-0.003	-0.008	2.407	-0.006	-0.008	2.259	-0.011	-0.008
$5p_{1/2} - 8d_{3/2}$	3.454	$\sim$0	$\sim$0	2.595	-0.013	-0.020	2.882	-0.022	-0.020	2.925	-0.028	-0.018
$5p_{3/2} - 7d_{5/2}$	5.667	$\sim$0	$\sim$0	5.747	-0.027	-0.018	6.365	-0.039	-0.018	5.827	-0.031	-0.018
$5p_{3/2} - 8d_{5/2}$	7.054	$\sim$0	$\sim$0	5.749	-0.048	-0.037	6.267	-0.071	-0.037	6.207	-0.057	-0.035
$\sum_{n,m}(ns - mp_{1/2})$	0.013	0.121	0.029	0.049	0.142	0.036	0.046	0.144	0.036	0.046	0.152	0.038
$\sum_{n,m}(ns - mp_{3/2})$	0.010	$\sim$0	0.036	0.025	0.003	0.042	0.018	0.003	0.042	0.037	0.004	0.048
$\sum_{n,m}(np_{1/2} - ms)$	1.064	0.326	0.078	1.382	0.500	0.136	1.532	0.529	0.136	1.474	0.466	0.122
$\sum_{n,m}(np_{3/2} - ms)$	3.183	$\sim$0	0.144	4.111	0.036	0.265	4.696	0.046	0.265	4.536	0.057	0.241
$\sum_{n,m}(np_{1/2} - md_{3/2})$	6.293	$\sim$0	-0.001	4.993	-0.022	-0.033	5.582	-0.038	-0.033	5.539	-0.047	-0.031
$\sum_{n,m}(np_{3/2} - md_{3/2})$	1.545	$\sim$0	$\sim$0	1.326	-0.003	-0.006	1.501	0.003	-0.006	1.375	-0.006	-0.007
$\sum_{n,m}(np_{3/2} - md_{5/2})$	13.860	$\sim$0	$\sim$0	11.887	-0.082	-0.064	13.428	-0.125	-0.064	12.871	-0.099	-0.060

CPHF contributions.

We present the contributions from the individual CCSD terms in Table II to highlight the importance of various correlation effects. It can be seen in this table that by far the most important contributions comes from $\overline{D}T_1^{(1)}$ term followed by $T_2^{(0)^\dagger}\overline{D}T_2^{(1)}$, where $\overline{D}$ is the effective one-body term of $\overbrace{D}$ and the contributions from the other terms are almost negligible. To carry out an analysis similar to the one given in [25], we find the contributions from various orbitals that correspond to various singly excited intermediate configurations for different properties which are given in Table III. These results are evaluated using the diagram shown in Fig. 2 with the corresponding $\Omega^{(1)}$ operator from the the DF, MBPT(2) containing diagrams that correspond only to the lowest order CPHF (denoted by MBPT(l-CPHF)), CPHF and CCSD methods. We also present the sum of contributions from the orbitals belonging to a particular category of angular momentum excitations to demonstrate their importance in obtaining the properties that have been calculated. The information provided in all the three tables together clearly expound the reasons for the different trends in the correlation effects in the calculations of α, η and ζ.

By combining our CCSD results for η and ζ with the available experimental limit for ^{129}Xe EDM, $d_a(^{129}\text{Xe}) < 4.1 \times 10^{-27}|e|cm$, we get the limits $C_T < 1.6 \times 10^{-6}$ and $S < 1.2 \times 10^{-9}\ |e|fm^3$. These are not superior to the limits extracted from ^{199}Hg [23, 28], which are about three orders of magnitude lower. However, the experiments on ^{129}Xe [13, 20, 21] that are underway have the potential to improve the current sensitivity by about three to four orders of magnitude. It therefore seems very likely that the best limits for both C_T and S could be obtained by combining our calculated values presented in this work and the results of the new generation of experiments for ^{129}Xe when they come to fruition. This limit for S in conjunction with the recent nuclear structure calculations [29] and quantum chromodynamics (QCD), would yield new limits for θ_{QCD} and CP violating coupling constants involving chromo EDMs of quarks.

We acknowledge useful discussions with Professor K. Asahi. This work was supported partly by INSA-JSPS under project no. IA/INSA-JSPS Project/2013-2016/February 28,2013/4098. The computations were carried out using the 3TFLOP HPC cluster at Physical Research Laboratory, Ahmedabad.

[1] I. B. Khriplovich and S. K. Lamoreaux, *CP violation without strangeness. Electric dipole moments of particles, atoms, and molecules*, (Springer, Berlin, 1997).
[2] B. L. Roberts and W. J. Marciano, *Lepton Dipole Moments, Advanced series on Directions in High Energy Physics*, vol. 20, World Scientific, Singapore (2010).
[3] G. Luders, Ann. Phys. (N.Y.) **281**, 1004 (2000).
[4] J. H. Christenson, J. W. Cronin, V. L. Fitch, and R. Turlay, Phys. Rev. Lett. **13**, 138 (1964).

[5] K. Abe *et al.*, Phys. Rev. Lett. **87**, 091802 (2001).
[6] B. Aubert *et al.*, Phys. Rev. Lett. **87**, 091801 (2001).
[7] R. Aaij *et al.*, Phys. Rev. Lett. **110**, 221601 (2013).
[8] M. Dine and A. Kusenko, Rev. Mod. Phys. **76**, 1 (2003).
[9] M. Pospelov and A. Ritz, Ann. Phys. (N.Y.) **318**, 119 (2005).
[10] S. M. Barr, Int. J. Mod. Phys. A **8**, 209 (1993).
[11] M. J. Ramsey-Musolf and S. Su, Phys. Rep. **456**, 1 (2008).
[12] T. Furukawa *et al.*, J. Phys. Conf. Ser. **312**, 102005 (2011).
[13] T. Inoue *et al.*, Hyperfine Interactions (Springer Netherlands) **220**, 59 (2013).
[14] E. T. Rand *et al.*, J. Phys. Conf. Ser. **312**, 102013 (2011).
[15] D. S. Weiss, Private communication.
[16] D. Heinzen, Private communication.
[17] S. M. Barr, Phys. Rev. D **45**, 4148 (1992).
[18] W. C. Griffith *et al.*, Phys. Rev. Lett. **102**, 101601 (2009).
[19] M. A. Rosenberry and T. E. Chupp, Phys. Rev. Lett. **86**, 22 (2001).
[20] P. Fierlinger *et al.*, *Cluster of Excellence for Fundamental Physics*, Technische Universität München (*http://www.universe-cluster.de/fierlinger/xedm.html*).
[21] U. Schmidt *et al. Collaboration of the Helium Xenon EDM Experiment*, Physikalisches Institut, University of Heidelberg (*http://www.physi.uni-heidelberg.de/Forschung/ANP/XenonEDM/T*
[22] A. Yoshimi *et al.*, Phys. Lett. A **304**, 13 (2002).
[23] V. A. Dzuba, V. V. Flambaum and S.G. Porsev, Phys. Rev. A **80**, 032120 (2009).
[24] A. M. Mårtensson-Pendrill, Phys. Rev. Lett. **54**, 1153 (1985).
[25] K. V. P. Latha and P. R. Amjith, Phys. Rev. A **87**, 022509 (2013).
[26] U. Hohm and K. Kerl, Mol. Phys. **69**, 819 (1990).
[27] Y. Singh, B. K. Sahoo and B. P. Das, Phys. Rev. A **88**, 062504 (2013).
[28] K. V. P. Latha, D. Angom, B. P. Das and D. Mukherjee, Phys. Rev. Lett. **103**, 083001 (2009).
[29] N. Yoshinaga, K. Higashiyama, R. Arai and E. Teruya, Phys. Rev. C **87**, 044332 (2013).